AE4304 Practical

Display of simulated aircraft responses to atmospheric turbulence

4667638 Tzanetos, George

April 10, 2022

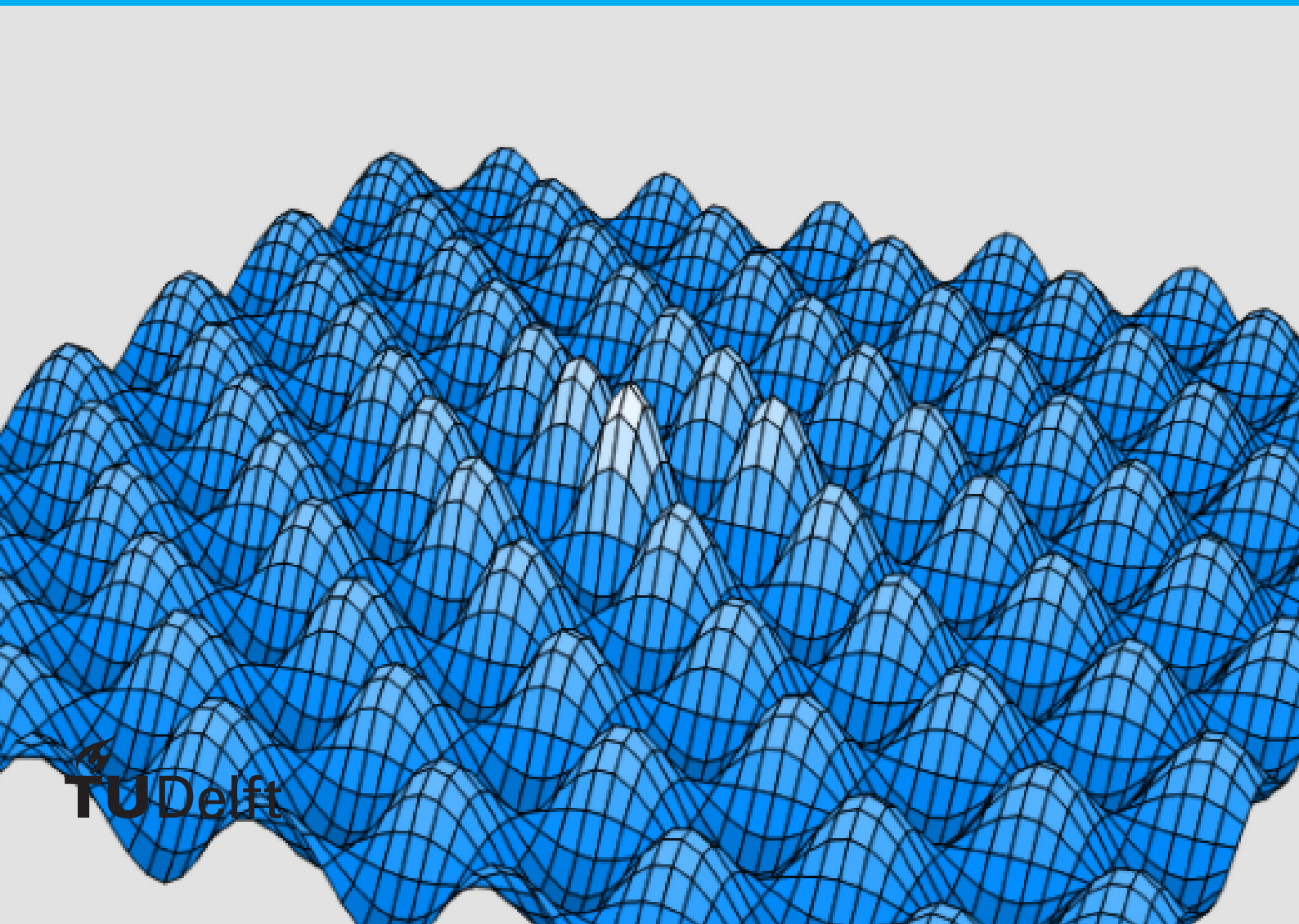

TU Delft

Contents

1

Introduction

Typically, most airline passengers have at some point experience turbulence of some level of intensity. What occurs is simply the encounter of disrupted air or air gaps by the aircraft. Although subtle mostly, they are essentially very powerful inputs to the aircraft's movement considering the cruise and mass it has. Nevertheless, it is one of the exciting projects for control engineers, as it is something completely unexpected, but excites them to make the control system of the aircraft as robust as possible. This assignment models the response and efficiency of performance, of an aircraft flying under specific conditions and under a specific set of turbulence input. More specifically, the turbulence conditions given for the assignment, are listed below:

- $L_g = 150m$
- $\sigma_{v_g} = 1m/s$
- $\sigma_{w_g} = 1m/s$

That is, there is simultaneously lateral and vertical turbulence input. Furthermore, the procedure follows the Dryden Power Spectral model. Initially, the first step that follows, will be the analysis of the stability of the model. The initial layout of the system is in state-space form, which is the result of simplification of the complicated equations of motions in the Flight Dynamics lectures [1]. Concerning the relation of the aircraft system with the turbulence input, it is brought to mathematical form by way of the Aircraft Responses to Turbulence lecture notes [2]. It should be obvious that before there is any simulation there must be stability check and if that does not exist everywhere, there should be controlling action. Moreover, there will happen simulations in the time and frequency domain. There exist two different models that serve the purpose to not only compare the methods of simulation, but also these two models. The second one, is a step further into simplification, from the initial one. Specifically, it concerns the equations of motion of the Dutch roll and aperiodic roll motion. The changes are as follows:

- $\beta = -\psi$
- $\phi \neq 0$

After time-response simulation, what will follow is spectral analysis using the analytical method, the Discrete Fourier Transform, and the special, smoothened case of it by Peter Welch. The results will also be discusses, since two models through three calculation methods are compared. Lastly, the variances will be calculated, and again through different methods, in order to provide ground for comparison, and the report will be completed with a concluding statement.

2

Stability Analysis

In this first part, the preliminary setup of the problem is introduced. That is, the model of the aircraft under turbulence input is derived through the simplified, linear Equations of Motion. As visible by the name of this chapter, the stability analysis of this model will be performed. This will be done for two different model versions, the primary one, and the reduced one afterwards. The state-space representation these follow is given by Equation 2.1, while the states and inputs are listed below in vectors 2.2 and 2.3, respectively.

$$\frac{d}{dt}\mathbf{X} = \mathbf{AX} + \mathbf{BU} \tag{2.1}$$

where

$$\mathbf{X} = \begin{bmatrix} \beta & \phi & \frac{pb}{2V} & \frac{rb}{2V} & \hat{u}_g & \hat{u}_g^* & \alpha_g & \alpha_g^* & \beta_g & \beta_g^* \end{bmatrix} \tag{2.2}$$

$$\mathbf{U} = \begin{bmatrix} \delta_\alpha & \delta_r & w_1 & w_3 & w_2 \end{bmatrix} \tag{2.3}$$

The control input vector includes the two deflections of the aileron and rudder, as well as the three directional components of the turbulence input. The matrices **A** and **B** that complete the representation are given below.

$$\mathbf{A} = \begin{bmatrix} y_\beta & y_\phi & y_p & y_r & 0 & 0 & 0 & 0 & y_{\beta_g} & 0 \\ 0 & 0 & 2\frac{V}{b} & 0 & 0 & 0 & 0 & 0 & 0 & 0 \\ l_\beta & 0 & l_p & l_r & l_{u_g} & 0 & l_{\alpha_g} & 0 & l_{\beta_g} & 0 \\ n_\beta & 0 & n_p & n_r & n_{u_g} & 0 & n_{\alpha_g} & 0 & n_{\beta_g} & 0 \\ 0 & 0 & 0 & 0 & 0 & 1 & 0 & 0 & 0 & 0 \\ 0 & 0 & 0 & 0 & -(\frac{V}{L_g})^2\frac{1}{\tau_1\tau_2} & -\frac{\tau_1+\tau_2}{\tau_1\tau_2}(\frac{V}{L_g}) & 0 & 0 & 0 & 0 \\ 0 & 0 & 0 & 0 & 0 & 0 & 0 & 1 & 0 & 0 \\ 0 & 0 & 0 & 0 & 0 & 0 & -(\frac{V}{L_g})^2\frac{1}{\tau_4\tau_5} & -\frac{\tau_4+\tau_5}{\tau_4\tau_5}(\frac{V}{L_g}) & 0 & 0 \\ 0 & 0 & 0 & 0 & 0 & 0 & 0 & 0 & 0 & 1 \\ 0 & 0 & 0 & 0 & 0 & 0 & 0 & 0 & -(\frac{V}{L_g})^2 & -2\frac{V}{L_g} \end{bmatrix} \tag{2.4}$$

$$\mathbf{B} = \begin{bmatrix} 0 & y_{\delta_r} & 0 & 0 & 0 \\ 0 & 0 & 0 & 0 & 0 \\ l_{\delta_\alpha} & l_{\delta_r} & 0 & 0 & 0 \\ n_{\delta_\alpha} & n_{\delta_r} & 0 & 0 & 0 \\ 0 & 0 & \frac{\tau_3}{\tau_1\tau_2}\sqrt{\frac{V}{L_g}I_{\hat{u}_g}(0,B)} & 0 & 0 \\ 0 & 0 & (1-\frac{\tau_3(\tau_1+\tau_2)}{\tau_1\tau_2})\frac{1}{\tau_1\tau_2}\sqrt{(\frac{V}{L_g})^3 I_{\hat{u}_g}(0,B)} & 0 & 0 \\ 0 & 0 & 0 & \frac{\tau_6}{\tau_4\tau_5}\sqrt{\frac{V}{L_g}I_{\alpha_g}(0,B)} & 0 \\ 0 & 0 & 0 & (1-\frac{\tau_6(\tau_4+\tau_5)}{\tau_4\tau_5})\frac{1}{\tau_4\tau_5}\sqrt{(\frac{V}{L_g})^3 I_{\alpha_g}(0,B)} & 0 \\ 0 & 0 & 0 & 0 & \sigma_{\beta_g}\sqrt{\frac{3V}{L_g}} \\ 0 & 0 & 0 & 0 & (1-2\sqrt{3})\sigma_{\beta_g}\sqrt{(\frac{3V}{L_g})^3} \end{bmatrix}$$

(2.5)

Substitution of the specific given constants for this assignment yields Equation 2 and Equation 2.7.

$$\mathbf{A} = \begin{bmatrix} -0.1464 & 0.1681 & -0.0129 & -7.6310 & 0 & 0 & 0 & 0 & -0.1464 & 0 \\ 0 & 0 & 7.6946 & 0 & 0 & 0 & 0 & 0 & 0 & 0 \\ -0.3214 & 0 & -1.5953 & 1.2720 & -0.9128 & 0 & -1.2768 & 0 & -0.3214 & 0 \\ 0.2851 & 0 & -0.1293 & -0.2934 & 0.0258 & 0 & -0.1085 & 0 & 0.2851 & 0 \\ 0 & 0 & 0 & 0 & 0 & 1 & 0 & 0 & 0 & 0 \\ 0 & 0 & 0 & 0 & -2.1368 & -4.0758 & 0 & 0 & 0 & 0 \\ 0 & 0 & 0 & 0 & 0 & 0 & 0 & 1 & 0 & 0 \\ 0 & 0 & 0 & 0 & 0 & 0 & -5.9411 & -6.7514 & 0 & 0 \\ 0 & 0 & 0 & 0 & 0 & 0 & 0 & 0 & 0 & 1 \\ 0 & 0 & 0 & 0 & 0 & 0 & 0 & 0 & -0.1174 & -0.6853 \end{bmatrix}$$

(2.6)

$$\mathbf{B} = \begin{bmatrix} 0 & 0.0449 & 0 & 0 & 0 \\ 0 & 0 & 0 & 0 & 0 \\ -1.0864 & 0.1037 & 0 & 0 & 0 \\ -0.0014 & -0.2281 & 0 & 0 & 0 \\ 0 & 0 & 0.0136 & 0 & 0 \\ 0 & 0 & -0.0442 & 0 & 0 \\ 0 & 0 & 0 & 0.0174 & 0 \\ 0 & 0 & 0 & -0.0911 & 0 \\ 0 & 0 & 0 & 0 & 0.0197 \\ 0 & 0 & 0 & 0 & -0.0096 \end{bmatrix} \quad (2.7)$$

Before any further moves, this system needs to be inspected for stability, calculating the eigenvalues. These are listed in the first column of Table 2.1. The third eigenvalue in line, shows a positive real part and represents an unstable spiral motion. The same, uncontrolled system is shown below, in Figure 2.1. It is also visible graphically, now, that the positive pole is unstable, and needs to be controlled by means of feedback gain.

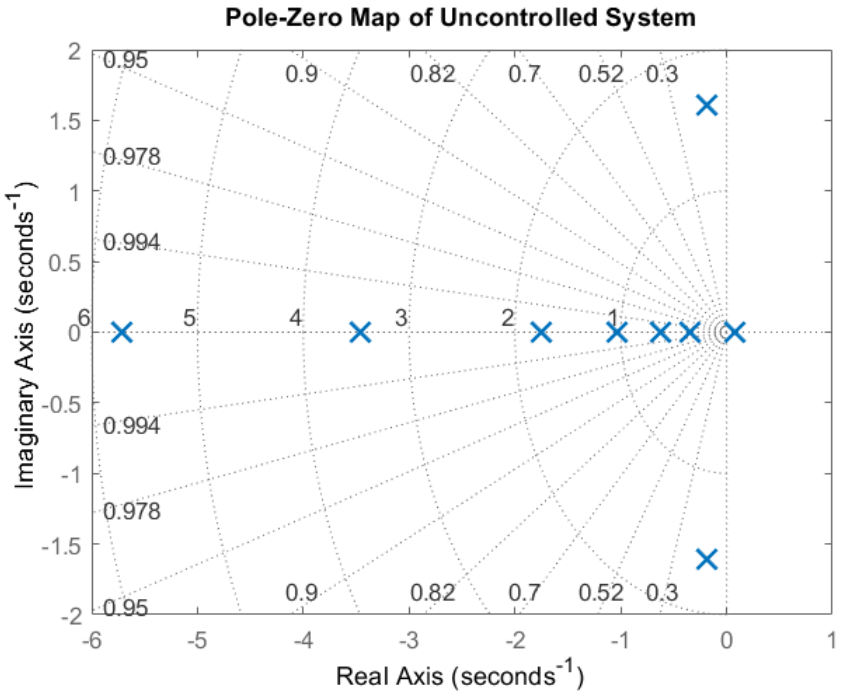

Figure 2.1: Pole-Zero map of uncontrolled system

The autopilotin design here is a roll damper, following the control law 2.8. After, tuning, the optimal gain values are chosen to be -0.1 and 0 for K_{phi} and K_p respectively. Repeating the plotting procedure, one gets to Figure 2.2, now having a successfully controlled system, and corresponding eigenvalues in column 2 of Table 2.1. This is the system that will be in use for the rest of this assignment regarding the full Equations of Motion, and the one to be compared with the reduced one in the simulation procedure.

$$\delta_\alpha = K_\phi \phi + K_p p \tag{2.8}$$

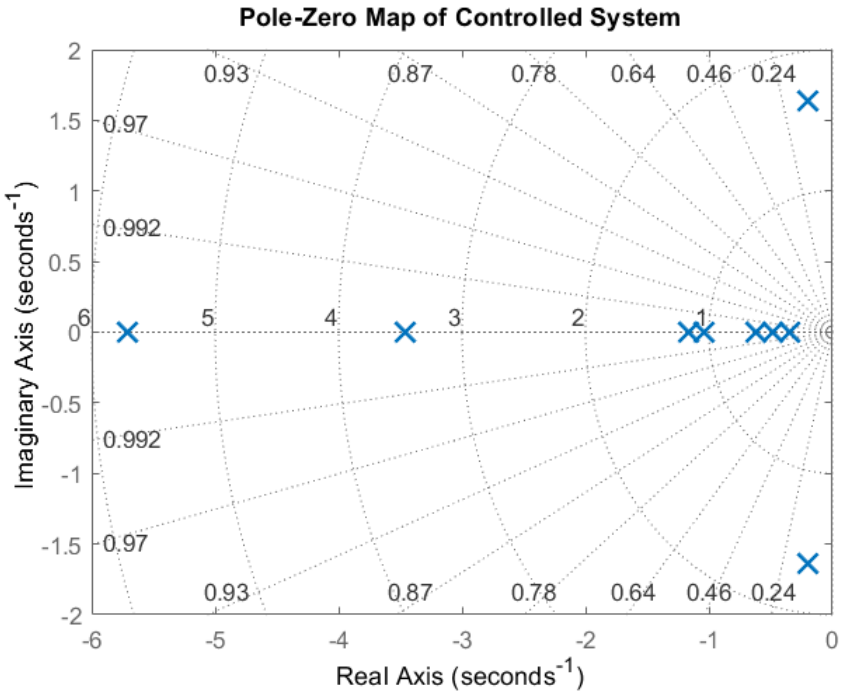

Figure 2.2: Pole-Zero map of controlled system

Regarding the reduced model, the following representations are given, shown in Equation 2.9.

$$\begin{aligned} \beta &= -\psi \\ \phi &\neq 0 \end{aligned} \tag{2.9}$$

For the sake of clarity, it is fairly obvious that the new system does not shorten in states. Throughout this whole assignment, and the MatLab code, the new system is referred to as ”reduced”, when it really is a Dutch-and-aperiodic-roll-representative system. The state vector therefore, remains the same as 2.2. The reduced system state-space follows from from the linearized ’deviation equation’ for the assymetric aircraft motions[1]. The objective now becomes to rid the system from the differential operator D_b the terms containing which are transferred to the right hand side, and the matrix equation becomes of the form:

$$\dot{\mathbf{x}} = \mathbf{P^{-1}Qx} + \mathbf{P^{-1}Ru} = \mathbf{Ax} + \mathbf{Bu} \tag{2.10}$$

with the matrices $\mathbf{P}, \mathbf{Q}$ and $\mathbf{R}$ described as follows[1]:

$$\mathbf{P} = \begin{bmatrix} b/2V & 0 & 0 & 0 \\ 0 & -b/2V & 0 & 0 \\ 0 & 0 & -4\mu_b {K_X}^2 b/V & 4\mu_b K_{XZ} b/V \\ 0 & 0 & 4\mu_b {K_{XZ}}^2 b/V & -4\mu_b {K_Z}^2 b/V \end{bmatrix}$$

(2.11)

$$\mathbf{Q} = \begin{bmatrix} 0 & 0 & 0 & -1 \\ 0 & 0 & -1 & 0 \\ -C_{l_\beta} & 0 & -C_{l_p} & -C_{l_r} \\ -C_{n_\beta} & 0 & -C_{n_p} & -C_{n_r} \end{bmatrix}$$

(2.12)

$$\mathbf{R} = \begin{bmatrix} 0 & 0 \\ 0 & 0 \\ -C_{l_{\delta_a}} & -C_{l_{\delta_r}} \\ -C_{n_{\delta_a}} & -C_{n_{\delta_r}} \end{bmatrix}$$

(2.13)

After Equation 2.10, one is left with the 4x4 $\mathbf{A}$ and $\mathbf{B}$ matrices, regarding only the 4 aircraft states. When the contribution of the gust states are concatenated on the right and underneath as two additional matrices, following the same equations as 2, and 2.7, the resulting matrices for $\mathbf{A_{red}}$ and $\mathbf{B_{red}}$, are obtsined below.

$$\mathbf{A_{red}} = \begin{bmatrix} 0 & 0 & 0 & -7.6946 & 0 & 0 & 0 & 0 & 0 & 0 \\ 0 & 0 & 7.6946 & 0 & 0 & 0 & 0 & 0 & 0 & 0 \\ -0.3214 & -0.1086 & -1.5953 & 1.2720 & -0.9128 & 0 & -1.2769 & 0 & -0.3214 & 0 \\ 0.2851 & 0 & -0.1293 & -0.2934 & 0.0258 & 0 & -0.1085 & 0 & 0.2851 & 0 \\ 0 & 0 & 0 & 0 & 0 & 1 & 0 & & 00 & 0 \\ 0 & 0 & 0 & 0 & -2.1368 & -4.0758 & 0 & 0 & 0 & 0 \\ 0 & 0 & 0 & 0 & 0 & 0 & 0 & 1 & 0 & 0 \\ 0 & 0 & 0 & 0 & 0 & 0 & -5.9411 & -6.7514 & 0 & 0 \\ 0 & 0 & 0 & 0 & 0 & 0 & 0 & 0 & 0 & 1 \\ 0 & 0 & 0 & 0 & 0 & 0 & & 0 & 0 - 0.1174 & 0.6853 \end{bmatrix}$$

(2.14)

$$\mathbf{B_{red}} = \begin{bmatrix} 0 & 0 & 0 & 0 & 0 \\ 0 & 0 & 0 & 0 & 0 \\ -1.0864 & 0.1037 & 0 & 0 & 0 \\ -0.0014 & -0.2281 & 0 & 0 & 0 \\ 0 & 0 & 0.0136 & 0 & 0 \\ 0 & 0 & -0.0442 & 0 & 0 \\ 0 & 0 & 0 & 0.0174 & 0 \\ 0 & 0 & 0 & -0.0911 & 0 \\ 0 & 0 & 0 & 0 & 0.0197 \\ 0 & 0 & 0 & 0 & -0.0096 \end{bmatrix} \tag{2.15}$$

Stability analysis here shows a stable system, however a roll-damper autopilot will help track the system of complete Equations of Motion more successfully, since one was implemented there. The same control law is used (2.8), and the optimal gains are chosen to be also -0.1 and 0 for K_{phi} and K_p, respectively. Once again, the again values can be seen in the last column of Table 2.1, and the pole-zero map below.

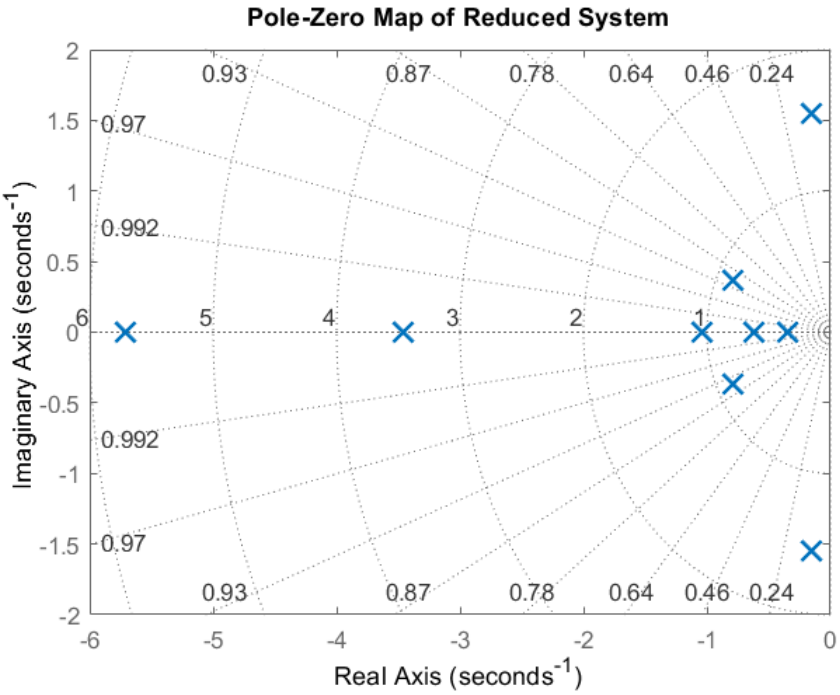

Figure 2.3: Pole-Zero map of reduced system

Table 2.1: Eigenvalues of the 3 systems and the corresponding eigenmotions

Mode	Uncontrolled System	Controlled System	Reduced System
Dutch Roll	-0.1826 + 1.6032i -0.1826 - 1.6032i	-0.1974 + 1.6349i -0.1974 - 1.6349i	-0.1523 + 1.5484i -0.1523 - 1.5484i -0.7920 + 0.3623i -0.7920 - 0.3623i
Spiral Motion	0.0763 + 0.0000i -0.3427 + 0.0000i -0.3427 + 0.0000i -0.6180 + 0.0000i -1.0403 + 0.0000i -1.7462 + 0.0000i	-0.3427 + 0.0000i -0.3427 + 0.00001 -0.4799 + 0.0000i -0.6180 + 0.0000i -1.0403 + 0.0000i -1.1605 + 0.0000i	-0.3427 + 0.0000i -0.3427 + 0.0000i -0.6180 + 0.0000i -1.0403 + 0.0000i
Highly Damped Aperiodic Roll	-3.4578 + 0.0000i -5.7111 + 0.0000i	-3.4578 + 0.0000i -5.7111 + 0.0000i	-3.4578 + 0.0000i -5.7111 + 0.0000i

3

Time-Domain Simulations

This chapter now simulates the aircraft's response to atmospheric turbulence and the performance of the models following the stability analysis displayed in chapter 2. Previously, only one of the two relations of the state-space representation is in Equation 2.1. The output equation is Equation 3.1.

$$\mathbf{Y} = \mathbf{CX} + \mathbf{DU} \tag{3.1}$$

Additionally, the gust states are now neglected for the simulation process, and the lateral acceleration is required to be simulated. It can be derived from existing states, with Equation 3.2.

$$a_y = \frac{d}{dt} V sin(\beta + \psi) \approx V(\dot{\beta} + \dot{\psi}) \tag{3.2}$$

In total, the outputs considered for this simulation are $\beta, \phi, \frac{pb}{2V}, \frac{rb}{2V}, a_y$. As mentioned, this particular assignment has simultaneous lateral and vertical turbulence as inputs. For those, the MatLab function *randn.m* is used, which is a pseudo-random of normally distributed numbers, to simulate a Gaussian white noise turbulence input. The resulting **C** and **D** matrices for both systems are given below, with the last rows representing Equation 3.2, and the rest containing the correction for degrees representation.

$$\mathbf{C} = \begin{bmatrix} 180/\pi & 0 & 0 & 0 & 0 & 0 & 0 & 0 & 0 & 0 \\ 0 & 180/\pi & 0 & 0 & 0 & 0 & 0 & 0 & 0 & 0 \\ 0 & 0 & 180/\pi & 0 & 0 & 0 & 0 & 0 & 0 & 0 \\ 0 & 0 & 0 & 180/\pi & 0 & 0 & 0 & 0 & 0 & 0 \\ Vy_\beta & Vy_\phi & By_p & V(y_r + (\frac{2V}{b}) & 0 & 0 & 0 & 0 & Vy_{\beta_g} & 0 \end{bmatrix} \tag{3.3}$$

$$\mathbf{D} = \begin{bmatrix} 0 & 0 & 0 & 0 & 0 \\ 0 & 0 & 0 & 0 & 0 \\ 0 & 0 & 0 & 0 & 0 \\ 0 & 0 & 0 & 0 & 0 \\ 0 & y_{\delta_r} & 0 & 0 & 0 \end{bmatrix} \tag{3.4}$$

Substitution of the specific given constants for this assignment yields:

$$\mathbf{C} = \begin{bmatrix} 57.2958 & 0 & 0 & 0 & 0 & 0 & 0 & 0 & 0 & 0 \\ 0 & 57.2958 & 0 & 0 & 0 & 0 & 0 & 0 & 0 & 0 \\ 0 & 0 & 57.2958 & 0 & 0 & 0 & 0 & 0 & 0 & 0 \\ 0 & 0 & 0 & 57.2958 & 0 & 0 & 0 & 0 & 0 & 0 \\ -7.5267 & 8.6402 & -0.6617 & 3.2705 & 0 & 0 & 0 & 0 & -7.5267 & 0 \end{bmatrix} \tag{3.5}$$

$$\mathbf{D} = \begin{bmatrix} 0 & 0 & 0 & 0 & 0 \\ 0 & 0 & 0 & 0 & 0 \\ 0 & 0 & 0 & 0 & 0 \\ 0 & 0 & 0 & 0 & 0 \\ 0 & 0.0449 & 0 & 0 & 0 \end{bmatrix} \tag{3.6}$$

The simulated time-response of the two models to the atmospheric turbulence, is displayed in Figure 3.1

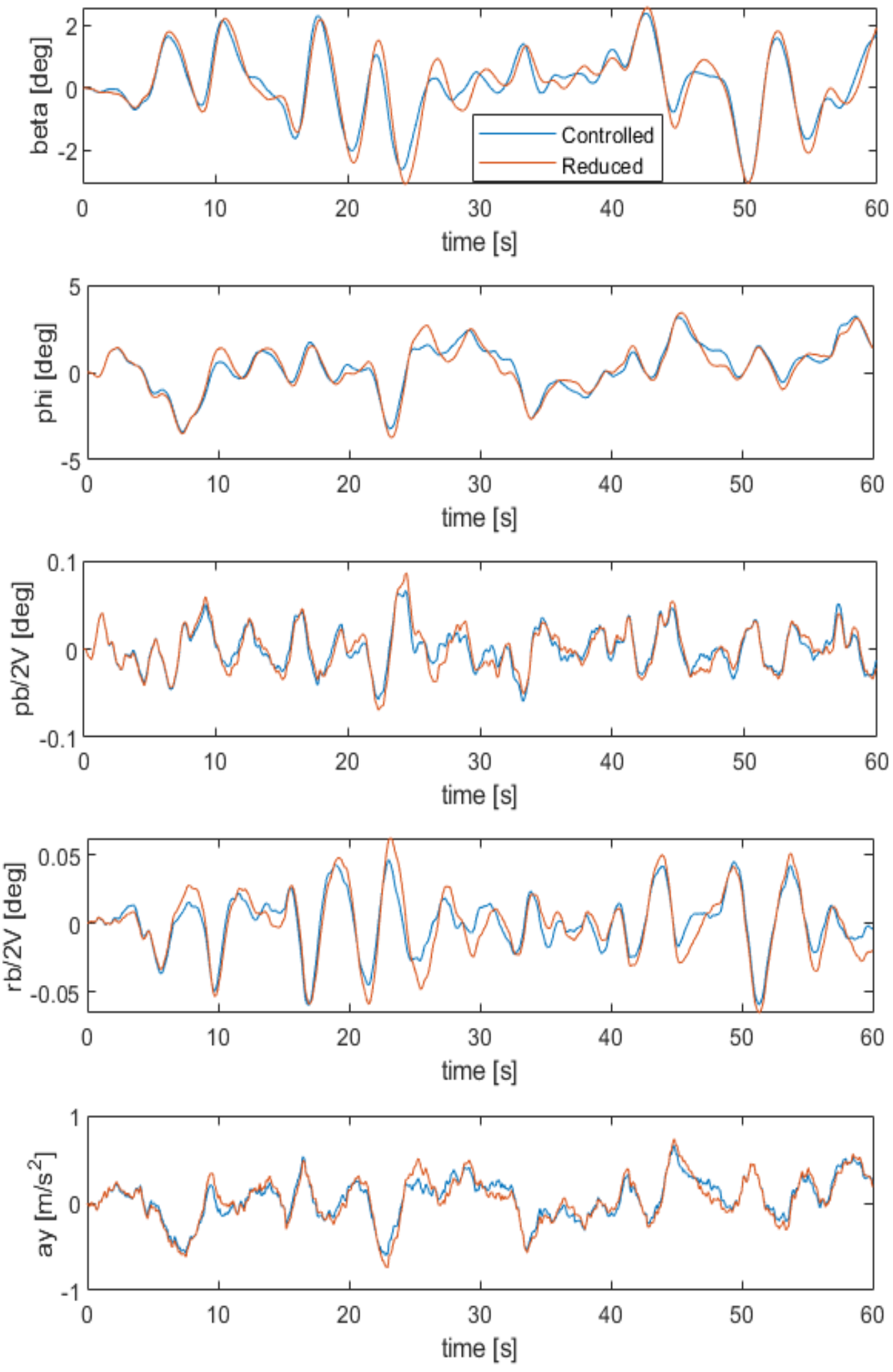

Figure 3.1: Time domain response of the two systems

4

Spectral Analysis

At this stage of the project, the Power Spectral Density is explored. The PSD plots refer to the distribution of the signal's power along a frequency spectrum. These are typically expressed in double-logarithmic scale graphs. Three different versions are examined for this report. Initially, the analytical PSD of the responses is derived from the magnitude of the frequency responses of the system through the $bode.m$ routine, G(ω). It is then used obtain the PSD through Equation 4.1.

$$S_{\omega\omega} = \lim_{T\to\infty} \frac{1}{2T}\left|G(\omega)\right|^2 \tag{4.1}$$

However the analytical PSD is deterministic and for simulations closer to real life one needs to explore experimental methods. This is why the other two PSD estimate methos are used. The first is by way of the MatLab $fft.m$ routine. Theoretically, The Discrete Fourier Transform (and so the Fast Fourier Transform too) is obtained using Equation 4.2.

$$\bar{X}[k] = \sum_{n=0}^{N-1} \bar{x}[n] e^{-jk\frac{2\pi}{N}n} \tag{4.2}$$

with both k and n ranging from 0 to N-1. Afterwards, the periodogram is given by Equation 4.3.

$$I_{N_{xx}}[k] = \frac{\left|\bar{X}[k]\right|^2}{N} \tag{4.3}$$

Finally, the second experimental method explored is by using the MatLab $pwelch.m$ routine, that uses Peter Welches method of PSD estimations, a smoothened DFT with modified periodograms of overlapping segments. A windowing function $w[n]$ is added to the sum of Equation 4.2 after partitioning the data.

$$I_{N_{xx}}[k] = \frac{\left|\bar{X}[k]\right|^2}{W} \quad \text{where} \quad W = \sum_{n=0}^{N} w^2[n] \tag{4.4}$$

The plot matrix in the following page organizes 30 lines in Bode plots, throughout 3 columns (one for each of the above methods), 5 rows (one for each state), and 2 plots in each window (one for each system). In the analytical section one sees the theoretical frequency response of the 5 states to atmospheric turbulence, and an excellent matching result of the "reduced" system, in comparison with the full Equations of Motion one. In the experimental part, the fft.m produces very different, and much more realistic spectra. In the states β, ϕ, a_y and in their higher frequencies (order of $10^{1.5}$), an error of size up to 10 $deg^2 s$ is present. This can be attributed to be inversely proportional to the sampling time $Deltat$ (see [2]) which is taken to be 0.05s in this simulation. However, this dissappears with the $pwelch.m$ routine, as well as the general noise in the higher frequencies thanks to the windowing function of the weight coefficients, described above in Equation 4.4. Finally, note that the units of the omega axes are rad/s.

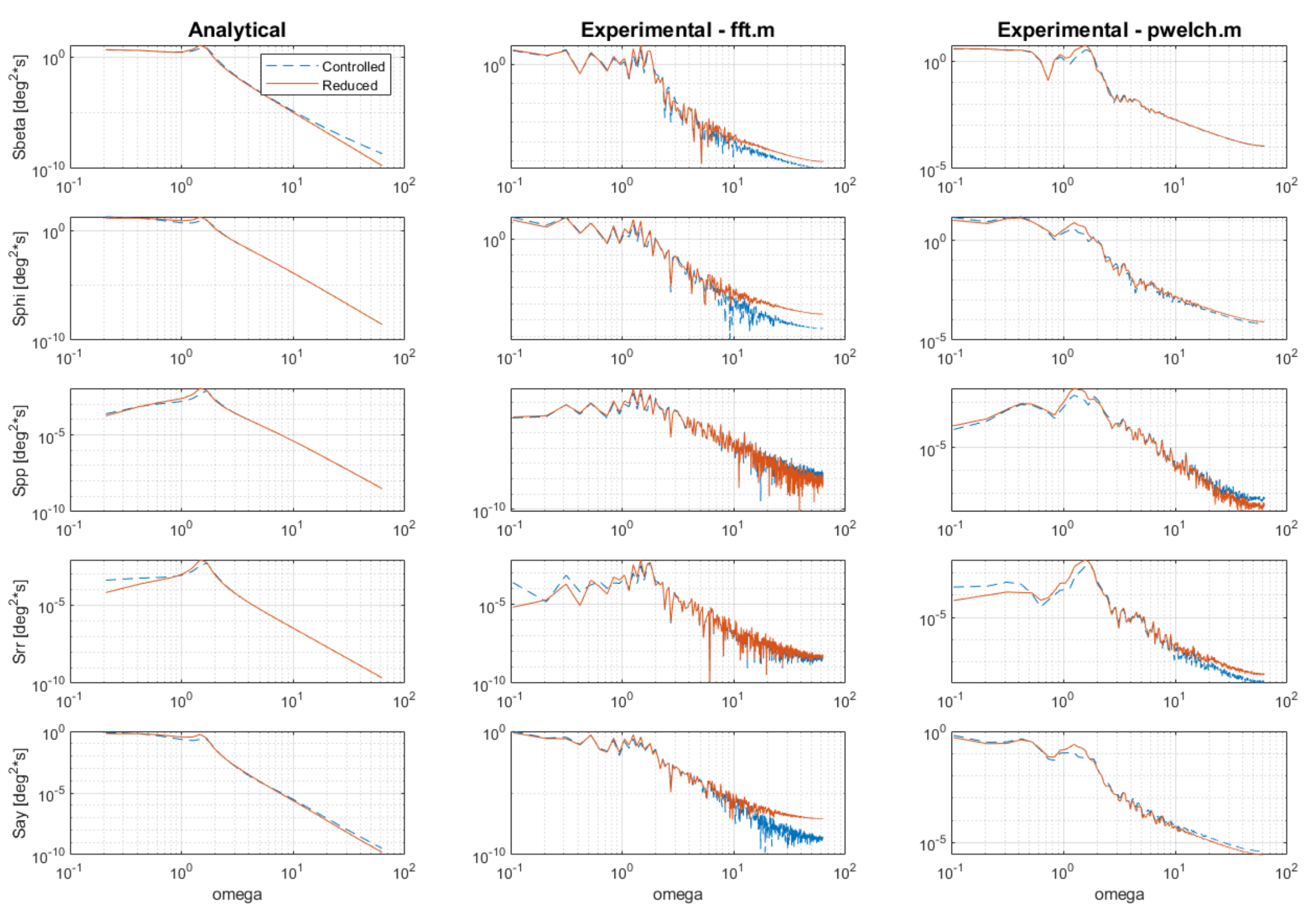
Analytical
Experimental - fft.m
Experimental - pwelch.m
Controlled
Reduced
Sbeta [deg^2*s]
Sphi [deg^2*s]
Spp [deg^2*s]
Srr [deg^2*s]
Say [deg^2*s]
omega
omega
omega

5

Variances

This final calculation chapter concerns variances. It is calculated using Equation 5.1.

$$\sigma^2 = \frac{1}{\pi}\int_0^\infty S(\omega)\, d\omega \tag{5.1}$$

with $S(\omega)$, the PSDs calculated in chapter 4 with all 3 methods (analytical, $fft.m$, $pwelch.m$) .In addition, the MatLab $var.m$ routine will be used. The method for this one can be seen below in Equation 5.2.

$$Var = \frac{1}{N-1}\sum_{i=1}^{N}\left|X_i - \mu_X\right| \tag{5.2}$$

As a result, the table underneath, Table 5.1 lists the resulting variances in the 4 capital columns, and distinguishes for the Controlled and Reduced system, labelled ”C” and ”R”, respectively in the subcolumns.

Table 5.1: Table of variances

	Analytical		**fft.m**		**pwelch.m**		**var.m**	
	C	**R**	**C**	**R**	**C**	**R**	**C**	**R**
β	2.7024	3.1156	3.0981	3.8373	2.8108	3.5385	1.5083	1.8760
ϕ	6.1807	6.8928	6.9017	7.5185	7.3902	7.8140	3.3462	3.6777
pb/2V	0.0018	0.0025	0.0016	0.0022	0.0015	0.0022	0.0008	0.0011
rb/2V	0.0010	0.0014	0.0011	0.0016	0.0010	0.0015	0.0005	0.0008
a_y	0.2564	0.2957	0.2372	0.2676	0.2465	0.2680	0.1128	0.1287

Firstly, the 3 columns corresponding to the 3 Power Spectra of chapter 4, are obviously representative of the Bode plots in the previous page. For the 5 states, the analytical variances show the least spread, followed by the pwelch.m ones, and the fft.m show the largest spread. Furthermore, the $var.m$ column displays signifincatly smaller values compared to all 3 others. This is attributed to the difference of the two aforementioned equations. As seen, this method uses the conventional discrete variance calculation, as opposed to the numerical integration performed for the rest. Finally, in every entry of the table, the variance for the reduced system exceeds the one for the controlled system. It is an intuitive result, if one considers the systems themselves. It has already been said that the latter is a simplified one, that approximates the lateral equations of motion. Even more, clearly, looking back at Figure 3.1, the reduced system successfully tracks the controlled one, but with larger swings at the peaks and dips. This makes it more prone to spread, and it produces a **higher variance** than the C-values in all instances, by average difference of **26.62%**.

6

Conclusion

To conclude with, as it was required by the title of this assignment, the report successfully took a dive into the practical version of all the delicate and complex techniques that are part of the Signal Processing world. Thankfully, the conditions for which this assignment should proceed were already laid down in a list, as constants, which is something that usually would require an assignment of its own. The aircraft model followed from simplified linear Equations of Motion [1] taking into account the desired inputs for the simulation $[\delta_\alpha, \delta_r, w1, w3, w2]$[2].

The stability analysis was firstly demonstrated. After setting up the state-space representation subject to the 10 states and 5 inputs, the eigenvalues were drawn up, together with the pole location in a pole-zero map. Initially there is a clear instability, consequently leading to unstable spiral eigenmotion. This is compensated by a roll damper autopilot described by the control law Equation 2.8, and using gains $K_{phi} = -0.1$ and $K_p = 0$.

These optimal gains produce time responses for the 5 aircraft states in chapter 3, after addition of state a_y, which is approximated with Equation 3.2. The reduced system successfully performs in following similar response to the same lateral and vertical turbulence as the controlled system. Moreover, it is time for the frequency spectrum response of the models. A matrix of Bode plots displayed the Power Spectral Density using 3 different methods. Firstly, analytically, and then experimentally ($fft.m$, and $pwelch.m$ routines). The Fast Fourier Transform estimate spectra show error in the larger frequencies of the response. This is related to time delay linked to the sampling time Δt[2], here chosen to be 0.05s. Compensation for this as well as smoothing is achieved with the Peter Welch method and its windowing function, explained in chapter 4. Overall, 300 samples are taken for the analytical spectra and 600 samples in the experimental ones. This assignment has showed its simulations and responses relative to state-space and gain parameters. A valid assumption for further examination is to keep these now constant and vary the simulation parameters previously mention.

Lastly, the variances are calculated in chapter 5. The first 3 capital columns of Table 5.1 are directly representative of the previous 30 spectra as they all follow the same numerical integration and scaling. The $var.m$ method was added to the chapter, which displays significantly smaller values, a result Equation 5.2 is responsible for. Lastly, the reduced system gives larger spread, by a factor of 1.266 compared to the controlled system. This is yet another indicator of successful imitation as an approximate system. The concluding assumption here is to explore the system's control further, and examine the similarity of the models after more a complex controller is applied for this assignments eigenmotions.

Bibliography

[1] W.H.J.J. van Staveren J.A. Mulder. Flight dynamics lecture notes, March 2013.

[2] W.H.J.J van Staveren Q.P. Chu M. Mulder J.A. Mulder, J.C. van der Vaart. Atmospheric responses to atmospheric turbulence: Lecture notes ae4304, November 2020.